

# Matter oscillations: Neutrino transformation in the Sun and regeneration in the Earth

A. J. Baltz and J. Weneser

*Physics Department, Brookhaven National Laboratory, Upton, New York 11973*

(Received 29 January 1988)

Calculations of neutrino regeneration phenomena in the Earth as well as transformation in the Sun are presented with relevant predictions for several existing and planned neutrino detection experiments. The validity of computational approximations in the solar case is appropriately investigated. Sensitivity of the calculated results to the solar model is noted. Transformation and regeneration phenomena are calculated to result from transmission through the Earth of neutrinos with  $E(\text{MeV})/\Delta m^2(\text{eV}^2)$  in the vicinity of  $10^6$  to  $10^7$ . As a result, large time-of-night and seasonal variations are predicted for various solar-neutrino experiments in this parameter range. Analogous effects are predicted for terrestrial cosmic-ray and accelerator experiments.

## I. INTRODUCTION

It was originally realized by Mikheyev and Smirnov<sup>1</sup> that resonant matter-induced neutrino oscillations could exist in the Sun and could provide a resolution of the "solar-neutrino puzzle" for a very wide range of the mass and mixing-angle parameters. That is, the effect of the solar medium on neutrinos emitted in the Sun's central region may well provide the basis for understanding the unexpectedly low counting rate observed in the BNL <sup>37</sup>Cl experiment.<sup>2</sup> Such an explanation implies a number of characteristic effects that are open to test in other experiments and would serve as clear confirmations of what we will call the Mikheyev-Smirnov-Wolfenstein (MSW) effect. As we have shown,<sup>3,4</sup> there is an analogous effect brought on by the neutrinos' passage through the Earth which also would lead to characteristic effects open to experimental test.

In this paper we carefully examine the effect of both the Sun's matter and the Earth's matter on the transformation of neutrinos from one species to another. Calculations of the MSW effect in the Earth are done numerically. While calculations of the MSW effect in the Sun can, for most regions, be carried out rapidly using the adiabatic and Landau-Zener approximations,<sup>5</sup> there has been some recent discussion questioning the validity of the Landau-Zener approximation in the case of large mixing angles and in case the neutrino source is near the resonance. As will be seen, we use alternate methods of computation in lieu of the Landau-Zener approximation when necessary. However, we do find that changes in solar-model parameters have a much larger effect on final results than do any calculational improvements over the Landau-Zener approximation.

Transmission effects within the Earth are dramatically large for some regions of the ratio of neutrino energy to the neutrino mass difference squared. In the appropriate parameter range such transmission phenomena translate into time-of-night and time-of-year effects for solar neutrinos that would be observable in real-time experiments. Depending on time resolution and statistics, such effects could appear as well in radio-chemical experiments.

Furthermore, our calculations show large effects for neutrinos created at the surface of the Earth and passing through it.

We begin our presentation in Sec. II with a general discussion of the computation of the Mikheyev-Smirnov-Wolfenstein effect in the Sun and in the Earth. In Sec. III we discuss the results of the BNL <sup>37</sup>Cl experiment in terms of the constraints it places on the neutrino mass and mixing angle. Significant changes in constraints are seen to accompany recent changes in the solar model.<sup>6</sup> Seasonal and day-night effects are considered. Predictions for the MSW effect on the <sup>71</sup>Ga solar-neutrino experiment are made, including a discussion of its complementarity to the <sup>37</sup>Cl experiment and the utility of seasonal and day-night effects in restricting the choice of parameters. The related phenomenon of matter-induced neutrino oscillations in the Earth for accelerator and cosmic-ray neutrinos is then treated in Sec. IV. In Sec. V the proposed detection of spectra of solar neutrinos in a real-time facility such as the Sudbury heavy-water detector is investigated with a detailed calculation of the predicted matter effects of the Earth. Finally, in Sec. VI some general remarks are made about the effect of the Earth on neutrino oscillations. Appendix A is concerned with the correctness of the omission of rapidly oscillating terms that correspond to phase oscillations on the long path from Sun to Earth. Appendix B presents a pedagogically explicit derivation of the transmission equation for neutrinos passing through matter, starting from an underlying Dirac equation.

## II. CALCULATING THE MSW EFFECT IN THE SUN AND EARTH

The basic equation describing the transmission through matter of neutrinos that can mix has been given by Wolfenstein.<sup>7</sup>

In the MSW formalism the general state, a mixture of the two neutrino species  $|\nu_e\rangle$  and  $|\nu_X\rangle$ ,

$$\Psi(t) = C_e(t) |\nu_e\rangle + C_X(t) |\nu_X\rangle$$

obeys the transmission equation

$$i \frac{d}{dt} \begin{bmatrix} C_e \\ C_X \end{bmatrix} = \begin{bmatrix} \frac{m_1^2}{2E} \cos^2 \theta + \frac{m_2^2}{2E} \sin^2 \theta + \sqrt{2} G_F n_e & \left[ \frac{m_2^2}{2E} - \frac{m_1^2}{2E} \right] \sin \theta \cos \theta \\ \left[ \frac{m_2^2}{2E} - \frac{m_1^2}{2E} \right] \sin \theta \cos \theta & \frac{m_2^2}{2E} \cos^2 \theta + \frac{m_1^2}{2E} \sin^2 \theta \end{bmatrix} \begin{bmatrix} C_e \\ C_X \end{bmatrix}. \quad (2.1)$$

The  $|\nu_e\rangle, |\nu_X\rangle$  are the particular combinations of the mass eigenstates  $|\nu_1\rangle$  and  $|\nu_2\rangle$  that couple to the  $\beta$  decay and other weak interactions; the  $\theta$  angle describes this fundamental mixing:

$$\begin{aligned} |\nu_e\rangle &= \cos \theta |\nu_1\rangle + \sin \theta |\nu_2\rangle, \\ |\nu_X\rangle &= -\sin \theta |\nu_1\rangle + \cos \theta |\nu_2\rangle. \end{aligned} \quad (2.2)$$

The  $\sqrt{2}G_F n_e$  represents the extra, charged-current interaction of the electron neutrino that acts over and above the interactions with electrons and nucleons that  $\nu_X$  would also have.

The transmission equation [Eq. (2.1)] is governed by the energy differences (for the same momenta) between the two mass components and by the interaction between the electron neutrino  $|\nu_e\rangle$ , and the electrons of the medium,  $\sqrt{2}G_F n_e$ —the part of the total interaction not available to the other neutrino species. The large mixing effects, the basis of the MSW phenomenon, occur at or near the degeneracy that occurs when the neutrino-electron interaction balances out the mass effects. This equality between the diagonal elements

$$\frac{m_1^2 - m_2^2}{2E} \cos 2\theta = -\sqrt{2}G_F n_e, \quad (2.3)$$

requires  $m_2 > m_1$  ( $\theta < \pi/4$  is understood), which we shall assume to be the case; in familiar units, this optimum mixing condition is

$$\frac{E(\text{MeV})}{\Delta m^2(\text{eV}^2)} \approx \frac{7 \times 10^6}{\rho(\text{g/cm}^3) y_e} \cos 2\theta, \quad (2.4)$$

where  $\rho$  is the density of the matter and  $y_e$  is the number of electrons per amu. Since the density of the Earth varies from  $\sim 3$  at the surface to  $\sim 13$  at the center<sup>8</sup> and  $y_e \sim \frac{1}{2}$ , neutrinos for which  $E/\Delta m^2$  lies in the region  $\sim 10^6$  to  $\sim 10^7$  should show interesting effects. Throughout this paper  $\Delta m^2$  will be stated in  $\text{eV}^2$ ,  $E$  in MeV.

For the full effects on solar neutrinos the transmission equation must be solved to obtain the amplitude on passage through the Sun and then, after travel through the vacuum between the Sun and Earth, through the Earth to the near-surface laboratory. The transmission through space is, of course, given by the simple free mass-eigenstate oscillation

$$\exp \left[ \frac{-i}{\hbar} \frac{m_1^2}{2E} t \right], \quad \exp \left[ \frac{-i}{\hbar} \frac{m_2^2}{2E} t \right].$$

The form of the flux that results from the complete transmission through the Sun, space, and Earth has been

written out in our previous paper.<sup>3</sup> Because of the free-state part of the transmission, terms that correspond to interference between the two mass state oscillations appear in the form

$$\exp \left[ \frac{i}{\hbar} \left[ \frac{m_2^2 - m_1^2}{2E} \right] t \right],$$

where  $t$  is the Earth-Sun separation. Since the parameter region of greatest interest is  $E(\text{MeV})/\Delta m^2(\text{eV}^2) \sim 10^6$  and the Earth-Sun separation is  $\sim 1.5 \times 10^{13}$  cm, the phase in these oscillating terms is seen to be  $\sim 2\pi(6 \times 10^4)$ . It is, then, clear that even a narrow binning of the observed energy spectrum suffices to make these interference oscillations negligible. In Appendix A, this is explicitly demonstrated to hold, even for the “monoenergetic” neutrino “lines” corresponding to electron capture, as for  $e^- + {}^7\text{Be} \rightarrow \nu + {}^7\text{Li}$ . Dropping the oscillation terms, the expression for the probability  $\bar{P}_{SE}$  that an electron neutrino emitted within the Sun remains an electron neutrino after passing through the Sun, the intermediate space, and the Earth is

$$\begin{aligned} \bar{P}_{SE} &= 1 + 2\bar{P}_S P_{E1} - \bar{P}_S - P_{E1} \\ &\quad - \frac{1}{2}(2\bar{P}_S - 1)(2P_{E2} - 1) \tan 2\theta. \end{aligned} \quad (2.5)$$

In this expression  $\bar{P}_S$  is the energy-averaged solution for the probability that an electron neutrino emitted in the Sun remains an electron neutrino if there were no Earth effect.  $P_{E1}$  is the probability that an electron neutrino created at one surface of the Earth will emerge at the other in the same condition;  $P_{E1}$  is, of course, a function of trajectory through the Earth.  $P_{E2}$  is the probability of finding an electron neutrino after a transmission that begins at the Earth’s surface with the boundary condition of a coherent mixture of equal parts of both species and with amplitudes in phase. The angle  $\theta$ , the mixing angle, is as defined earlier. The need for two transmission functions  $P_{E1}$  and  $P_{E2}$  is present only if the phase between the two components of the amplitude incoming on the Earth is relevant; in the present application where the interferences between the two components has been averaged to zero, a single function to represent effects of transmission through the Earth suffices—and this is the format that Mikheyev and Smirnov have chosen in their Moriond ’87 review;<sup>9</sup> since we wish to use the physically applicable  $P_{E1}$  we have preferred to also calculate  $P_{E2}$  rather than some other linear combination of Earth transmission functions.

It is important to note that the averaging is applicable only to solar transmission quantities; the Earth solutions

$P_{E1}$  and  $P_{E2}$  are kept exact functions of the trajectory from Earth entry to Earth exit or detector. The narrow energy averaging or spectrum binning used here would not change these Earth transmission functions appreciably.

A calculation of the solar MSW effect may, in general, be accurately carried out for a given set of parameters:  $\theta$ ,  $E/\Delta m^2$ , and a neutrino source position in the Sun. However, since all of these must be varied and then integrated over, the amount of computing time may become quite burdensome. Approximations offer a welcome relief. The adiabatic approximation when suitably ameliorated

by the Landau-Zener<sup>5</sup> approximate correction has served very usefully. Here we use Parke's<sup>5</sup> expression for the probability that an electron neutrino remains such after passing through the Sun:

$$\bar{P}_S = \frac{1}{2} + \left(\frac{1}{2} - P_x\right) \cos 2\theta \cos 2\theta_N. \quad (2.6)$$

Here  $\theta$  is the already defined mixing angle;  $\theta_N$  is the effective rotation between the weak-interaction states  $|\nu_e\rangle$ ,  $|\nu_x\rangle$  at the point of origin of the neutrinos and the matter-influenced eigenstates, the eigenstates of the mass-matter matrix given in Eq. (2.1):

$$\sin 2\theta_N = \sin 2\theta \frac{\frac{m_2^2 - m_1^2}{2E}}{\left[ \left( \frac{m_2^2 - m_1^2}{2E} \cos 2\theta - \sqrt{2} G n_e \right)^2 + \left( \frac{m_2^2 - m_1^2}{2E} \sin 2\theta \right)^2 \right]^{1/2}}. \quad (2.7)$$

If the matter effect vanishes,  $n_e = 0$ ,  $\theta_N = \theta$ ; for large values of  $n_e$ , as at the solar center,  $\theta_N \rightarrow \pi/2$ , and  $\cos 2\theta_N \rightarrow -1$ . Were the matter density a constant, the neutrino amplitude would be described as a linear combination of the matter eigenstates, with a phase given by the eigenvalue differences. In the actual case of a variable density, high at the center, zero at the surface, there are transitions between these matter eigenstates, and mostly so at the region where the difference in diagonal matrix elements vanishes, Eq. (2.3), "the resonance condition."  $P_x$  is the Landau-Zener probability for a transition between the matter eigenstates that occurs at and in the vicinity of the "resonance crossing":

$$P_x = \exp \left[ -\frac{\pi}{2} \frac{\sin^2 2\theta}{\cos 2\theta} \frac{(m_2^2 - m_1^2)/2E}{\hat{n} \cdot \nabla \ln n_e|_{\text{res}}} \right], \quad (2.8)$$

where the unit vector  $\hat{n}$  is the direction of propagation of the neutrino. Clearly if the resonance crossing is gradual,  $\hat{n} \cdot \nabla \ln n_e \rightarrow 0$  and  $P_x \rightarrow 0$ , and  $\bar{P}_S$  is given by the adiabatic (no transitions between the original population of the matter eigenstates) result.<sup>1</sup> If a neutrino is born downstream of the resonant density, and, therefore, does not cross the resonant region,  $P_x \rightarrow 0$ . A neutrino that originates at a point whose density is less than the resonant density, but whose direction of motion is inward, crosses the resonant density twice; in this case

$$P_x \rightarrow 2P_x(1 - P_x).$$

Nevertheless, it is sad to say that there are two regions of the  $\theta, E/\Delta m^2$  parameter space where perceptible inaccuracies may arise from the use of the above approximations. These inaccuracies are relatively small, amounting to slight displacements of contour lines in very limited regions of the parameter space. Haxton<sup>10</sup> has pointed out similar deficiencies in his parallel Landau-Zener treatment and presented a somewhat more accurate alternate

treatment. Other approaches to improving the analytical Landau-Zener result in this region include using an exponential density expansion rather than a linear one.<sup>11</sup> However, we will modify the adiabatic and Landau-Zener approximations by using exact numerical solutions in these regions to attain the requisite level of accuracy in the calculations.

The first region where the Landau-Zener approximation loses significant accuracy was pointed out by Haxton,<sup>10</sup> Petcov,<sup>12</sup> and by Toshev.<sup>13</sup> This is the region of large mixing angles and significant Landau-Zener correction to the adiabatic formula. Table I exhibits a comparison of Landau-Zener and exact numerical calculations in the region of interest. It should be pointed out in passing that the form of the Landau-Zener approximation used does not approach the correct vacuum result at high  $E/\Delta m^2$  as it is required to do. The vacuum result for  $\bar{P}_s$  is  $(\frac{1}{2} + \frac{1}{2} \cos^2 2\theta)$  while the Landau-Zener expression for  $\bar{P}_s$  approaches  $(\frac{1}{2} + \frac{1}{2} \cos 2\theta)$ . Clearly we will cover the region of lost accuracy if we use exact numerical integration for the region where both  $\sin 2\theta \geq 0.1$  and  $E/\Delta m^2 \geq 10^7$ . Of course, the resonant region becomes very broad in the high mixing angle limit. The numerical solution is not as time consuming in this region, however, since the point source approximation (source taken as confined to the solar center) can be made without loss of accuracy.

A second small troublesome region in which the Landau-Zener approximation loses its validity corresponds to the parts of the neutrino source near the resonance region; this has been analyzed by Mikheyev and Smirnov.<sup>9</sup> Two kinds of deviations between the exact calculations and the Landau-Zener calculations are apparent. The first is an oscillation about the Landau-Zener probability as a function of the distance of the point of origin from the resonance. A variation of this effect which we have discovered is a similar oscillation

TABLE I. Comparison of Landau-Zener (LZ) calculations with exact numerical calculations for neutrinos starting at the center of the Sun. Probability of remaining an electron neutrino is tabulated. In these calculations both the LZ and exact cases correspond to an exponential falloff of densities in the outer solar region.

$E/\Delta m^2$	$\sin 2\theta$	0.1	0.2	0.4	0.6	0.8	0.95
$10^7$	LZ	0.755	0.325	0.049	0.100	0.200	0.344
	Exact	0.756	0.329	0.051	0.100	0.200	0.344
$2.51 \times 10^7$	LZ	0.883	0.606	0.150	0.103	0.200	0.344
	Exact	0.884	0.613	0.166	0.106	0.200	0.344
$6.31 \times 10^7$	LZ	0.951	0.817	0.443	0.196	0.204	0.344
	Exact	0.951	0.818	0.457	0.224	0.218	0.346
$1.58 \times 10^8$	LZ	0.980	0.920	0.710	0.454	0.287	0.346
	Exact	0.979	0.920	0.718	0.487	0.343	0.371
$3.98 \times 10^8$	LZ	0.990	0.961	0.850	0.678	0.478	0.383
	Exact	0.990	0.960	0.849	0.690	0.524	0.450
$10^9$	LZ	0.995	0.978	0.913	0.803	0.642	0.480
	Exact	0.993	0.973	0.896	0.774	0.621	0.507

that depends on the distance between resonances in double-resonance crossing. We will ignore both these oscillations because energy averaging and source position variation tend to average them out.

The second deviation is more serious, and how it arises may be seen directly in the Landau-Zener formula for the case treated by Mikheyev and Smirnov: small values of  $\theta$  and large values of the Landau-Zener factor  $P_x$ . Here  $\cos 2\theta$  is approximately unity, and the probability formula becomes

$$\bar{P}_S \simeq \frac{1}{2} + \left(\frac{1}{2} - P_x\right) \cos(2\theta_N).$$

There is an obvious pathology when the neutrinos originate on a resonance,  $\cos 2\theta_N \sim 0$ , for then the relation requires  $\bar{P}_S \sim \frac{1}{2}$ , independent of  $P_x$ . We deal with this in a rather rough and ready fashion, because the contribution from this region is not large and because this small  $\theta$  region is far from that of a sizable Earth effect—the main point of this paper. If  $\sin 2\theta \leq 0.1$ , then we simply take (1)  $\cos 2\theta_N = 1$  for neutrinos that pass through either none or two resonances; that is, we take the low matter density limit. For no resonances  $P_x \rightarrow 0$ , while for the two resonance case we take  $2P_x(1 - P_x)$ . (2) For neutrinos that pass through one resonance we take  $\cos 2\theta_N = -1$ , the high matter density limit.

Figure 1(a) shows a calculation of  $\bar{P}_S$  for values of  $\sin 2\theta$  of 0.0125, 0.025, 0.05, 0.1, 0.2, and 0.4. The spatial distribution of the neutrino source is that calculated by Bahcall and Ulrich<sup>6</sup> as appropriate for  $^8\text{B}$ . The Landau-Zener solution has been used throughout except for our ansatz for neutrinos that originate near a resonance with  $\sin 2\theta \leq 0.1$  as discussed above. It is obvious from Table I that an exact calculation would change none of the curves noticeably (although we do use exact integration for  $\sin 2\theta \geq 0.1$  and  $E/\Delta m^2 \geq 10^7$  in the calculations to follow). The fact that the neutrino source may be approximated by a point in the center of the Sun for  $E/\Delta m^2 \geq 10^7$  becomes evident in the comparison of Fig. 1(a) with Fig. 1(b), the corresponding calculation of  $\bar{P}_S$  in which the spatial distribution is that of a  $p$ - $p$  (Ref. 6)

source of neutrinos. The  $^8\text{B}$  source is most pointlike, with only 5% of the neutrinos originating outside a solar radius of  $0.09R_\odot$ . The  $p$ - $p$  source, on the other hand, is the most diffuse, with 5% of the neutrinos originating outside a solar radius of  $0.21R_\odot$ . There is no perceptible difference between the two sets of curves for  $E/\Delta m^2 \geq 10^7$ . This is because at  $E/\Delta m^2 \geq 10^7$  and  $\cos 2\theta \approx 1$  the MSW resonance occurs beyond  $\approx 0.56R_\odot$  which is well outside the effective source region. For higher energy or larger mixing angle, the resonance is at an even larger radius, as is evident from Eq. (2.4) ( $n_e$  is decreasing with increasing distance from the center of the Sun). All the neutrinos originate inside the resonance, and only a very few cross it at an angle sufficiently off the radial to have any effective change from the radial case.

On the whole, the results of calculations more exact than the Landau-Zener result for the MSW effect in the Sun show fairly small differences from the Landau-Zener result. Approximations used in computing the MSW transformation have far less effect on the final result for the admissible values of the physical parameters,  $\Delta m^2$  and  $\theta$ , than the possible changes in two physics ingredients of the calculation: (1) the predicted neutrino flux, which together with that measured in the  $^{37}\text{Cl}$  experiment, determines the fractional diminution and (2) the radial shape of the electron density in the outer region of the Sun. This is borne out in the calculations presented here when compared with a corresponding preliminary set of calculations.<sup>14</sup> The preliminary calculations used Landau-Zener everywhere in the Sun with an exponential falloff in the Sun's outer region and an older set of solar parameters<sup>15</sup> corresponding to an expected detection of 5.8 solar-neutrino units (SNU) in the  $^{37}\text{Cl}$  experiment. The present calculations matched a power-law form (suggested by the convection mechanism that dominates this outer region) to the last electron-density point given by Bahcall and Ulrich for the outer region,

$$\rho = \rho(r_M = 0.914518) \left( \frac{1-r}{0.085482} \right)^{1.700974}, \quad r > 0.914518,$$

and used the latest solar parameters corresponding to an expected detection of 7.9 SNU in the  $^{37}\text{Cl}$  experiment. The power-law form changed contour shapes somewhat at  $\Delta m^2$  of about  $10^{-7}$ , while the changed solar fluxes of course had a large effect. Both overshadowed any improvements in accuracy over the Landau-Zener calculations.

As already noted for transmission through the Earth, direct numerical solution of the transmission equation (2.1) appears to be the most satisfactory way to get trustworthy results. The form of the first-order coupled

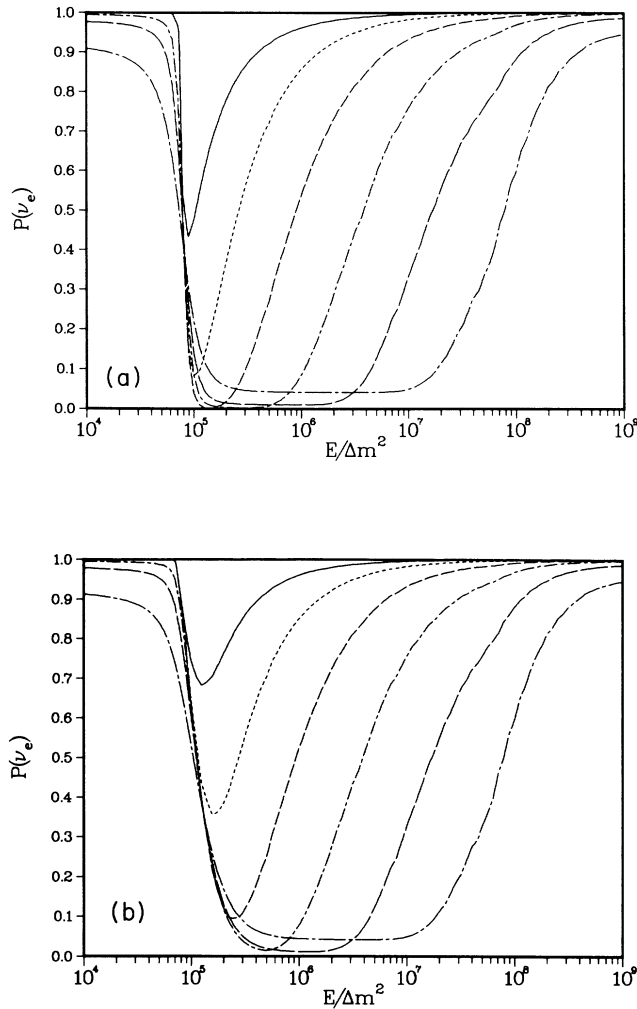


FIG. 1. A recalculation of the Mikheyev-Smirnov solution for the probability that an electron neutrino created in the central solar region will avoid an oscillation transformation and will survive as an electron neutrino in its transit through the solar medium and space to the Earth. Six values of the mixing parameter  $\sin^2 2\theta$  are shown: solid line, 0.0125; short-dashed line, 0.025; medium-dashed line, 0.05; medium-dashed-short-dashed line, 0.1; long-dashed line, 0.2; long-dashed-short-dashed line, 0.4. (a) corresponds to the spatial distribution of  $^8\text{B}$  solar neutrinos presented in Ref. 6, and (b) to the  $p$ - $p$  neutrino solar source distribution.

differential equations, as written by Mikheyev and Smirnov,<sup>1</sup> are solved using the Bashforth-Adams-Milne predictor-corrector method<sup>16</sup> in the Earth and in the Sun where numerical results are required as noted above.

### III. $^{37}\text{Cl}$ RESULTS AND THE $^{71}\text{Ga}$ EXPERIMENT

Since the data in the  $^{37}\text{Cl}$  experiment were taken night and day over a number of years, effects of the Earth would affect the count rate only in an average way. Figure 2(a) shows contour lines of the expected neutrino rate as detected by the  $^{37}\text{Cl}$  experiment as a function of the parameters  $\sin^2 2\theta/\cos 2\theta$  and  $\Delta m^2$ . The latest standard solar-model values<sup>6</sup> have been used for the strength and spatial distribution of the sources of neutrinos. This solar model predicts, in the absence of neutrino alteration effects, a rate of 7.9 SNU in the  $^{37}\text{Cl}$  experiment. (1 SNU =  $10^{-36}$  captures per target atom per second.) The effect of the Earth has been included in the calculation of the contours by averaging over day and night and seasonal changes for a year. For comparison, Fig. 2(b) displays the iso-SNU contours without the effect of the Earth. This plot is very similar to that originally presented by Parke and Walker<sup>5</sup> for the MSW effect on the Cl experiment without the effect of the Earth. In fact, using the same parameters and pure Landau-Zener calculations, our curves agreed with Parke and Walker<sup>5</sup> very well for this case.<sup>14</sup> If one interprets the  $^{37}\text{Cl}$  result of 2.1 SNU as due to a reduction from the expected 7.9 SNU because of matter oscillations, then it is evident that the set of points on the plot that are consistent with the experimental result is affected by the proper inclusion of the averaged effect of the Earth, especially in the region  $\sin^2 2\theta \gtrsim 0.1$ ;  $\Delta m^2 \approx 3 \times 10^{-4}$ . The so-called third solution, the near-vertical portion of the contour on the right of the plot, corresponds to a large mixing angle,  $\sin 2\theta$ , of about 0.87, without the effect of the Earth. On the other hand, the average effect of the Earth distorts the contour to  $\sin 2\theta$  under 0.6.

It is interesting to compare these calculations with calculations which differ only by using the previous predicted flux<sup>15</sup> of 5.8 SNU. Figure 3 shows a comparison of the  $\Delta m^2, \theta$  region allowed by a  $^{37}\text{Cl}$  result of  $2.1 \pm 0.3$  SNU when the latest solar parameters (leading to 7.9 SNU without MSW) are chosen with the region allowed if the previous solar parameters (5.8 SNU without MSW) are taken instead. There is practically no overlap between the regions allowed in the two different cases. In fact, if the new value were due only to a scaling up of all fluxes equally by  $7.9/5.8$  then the contours originally corresponding to  $2.1 \pm 0.3$  SNU would lie at the same location as those for  $2.9 \pm 0.4$  for the new solar model. Obviously, this is roughly what has happened. The effect of raising the calculated solar model fluxes is to push the triangular band of allowed values of  $\Delta m^2$  and  $\sin^2 2\theta/\cos 2\theta$  inward on all sides. The effect is particularly striking for the "third solution" (the near  $\Delta m^2$  independent band at the right-hand edge), where the old solar model allows only very large mixing angles ( $\sin 2\theta \approx 0.8-0.95$ ), while the newer solar model leads to a third solution consistent with intermediate mixing angles ( $\sin 2\theta \approx 0.6-0.87$ ).

In the following calculations we will, in general, present results using only the latest solar model of 7.9 SNU. It should be borne in mind, however, that changes as large as the latest change in the solar model (of 5.8 to 7.9 SNU) do change the detailed predictions for solar-neutrino experiments. Further examples of calculations with the previous solar model can be found in our preliminary report.<sup>14</sup>

For possible developmental purposes it is also of use to investigate the day-night difference in the number of counts expected in the  $^{37}\text{Cl}$  experiment. For simplicity we will present here the results for that part of the year when day and night are approximately equal in length, the 6 months closest to the two equinoxes. Night is taken to be 12 h; daytime is simply taken as 12 h, with no Earth effect. Figure 4 shows the difference between the number

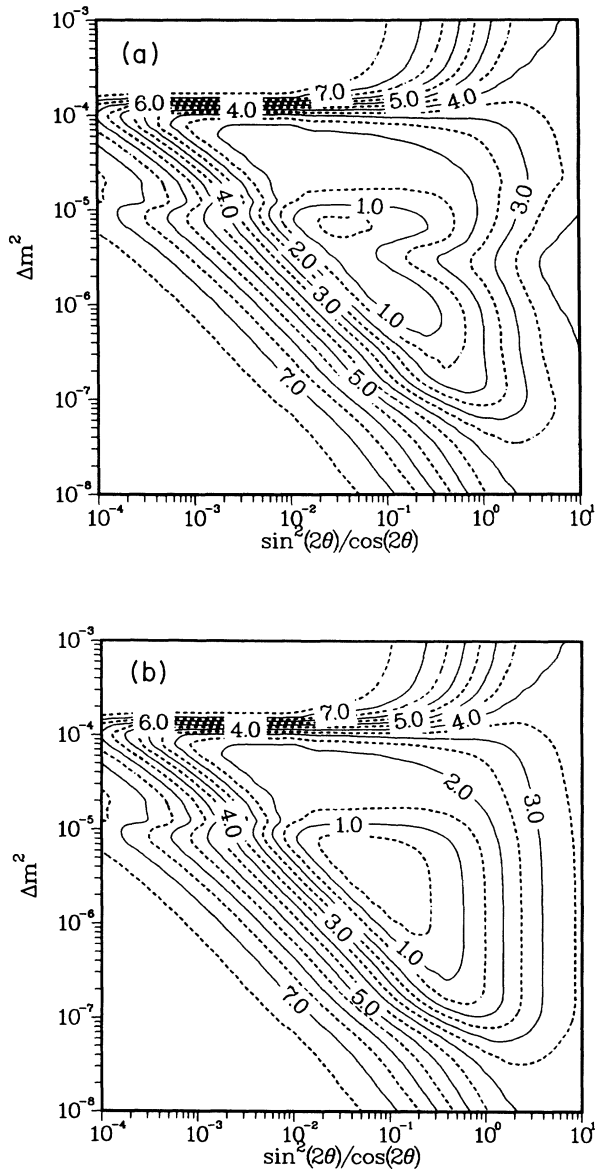


FIG. 2. Contours for the  $^{37}\text{Cl}$  experiment labeled by SNU values (see text). (a) includes the Earth effect, while (b) omits it.

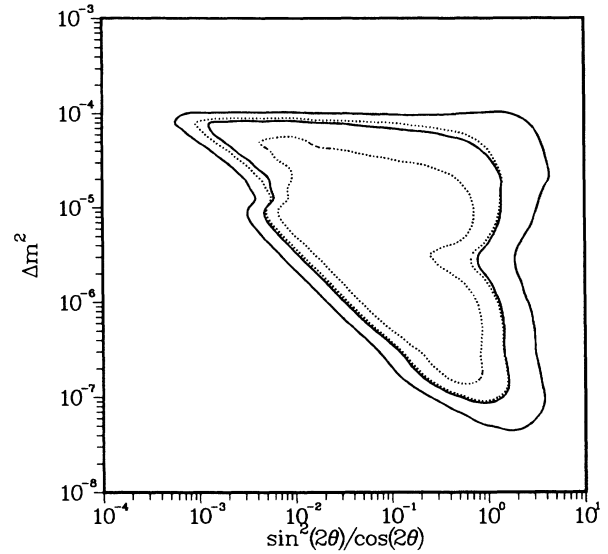


FIG. 3. Comparison of region allowed for  $2.1 \pm 0.35$  SNU by the latest (7.9 SNU) solar parameters (dotted contours) and by previous (5.8 SNU) solar parameters (solid contours). In both cases the allowed region is the band between the contours.

of counts seen at night and the number seen during the daytime. Superimposed is the band corresponding to the solutions valid for the existing data [Fig. 2(a)]. There is a region of the parameter space consistent with the existing data for which separate night-day measurements would show a detectable effect.

Experiments based on  $^{71}\text{Ga}$  are soon to be in operation.<sup>17</sup> The predicted response of the  $^{71}\text{Ga}$  detector is different from  $^{37}\text{Cl}$  mainly because of the lower-energy

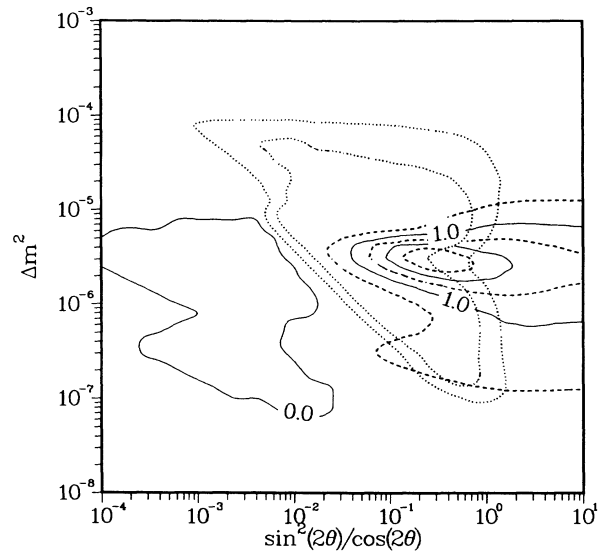


FIG. 4. Night minus day contours (solid) for the  $^{37}\text{Cl}$  experiment labeled by SNU values. The band between the dotted contours is the region consistent with the existing experimental result of  $2.1 \pm 0.3$  SNU.

neutrino threshold of the former. This allows  $^{71}\text{Ga}$  to detect the neutrinos from the basic  $p$ - $p$  burning process in the Sun that are inaccessible to  $^{37}\text{Cl}$ . Figures 5(a) and 5(b) show the contours of equal SNU's expected night and day, respectively, in the  $^{71}\text{Ga}$  experiment. The superimposed dotted band of the values consistent with the  $^{37}\text{Cl}$  experiment indicates compatibility with an experimental  $^{71}\text{Ga}$  result of anywhere from near zero to near the full solar-model prediction of about 133 SNU's.

If early results from the  $^{71}\text{Ga}$  experiment show a low number of counts relative to the solar-model prediction, then the night-day differences might well be worth measuring. Figure 6 shows the predicted difference in number of counts between night and day for  $^{71}\text{Ga}$ . The

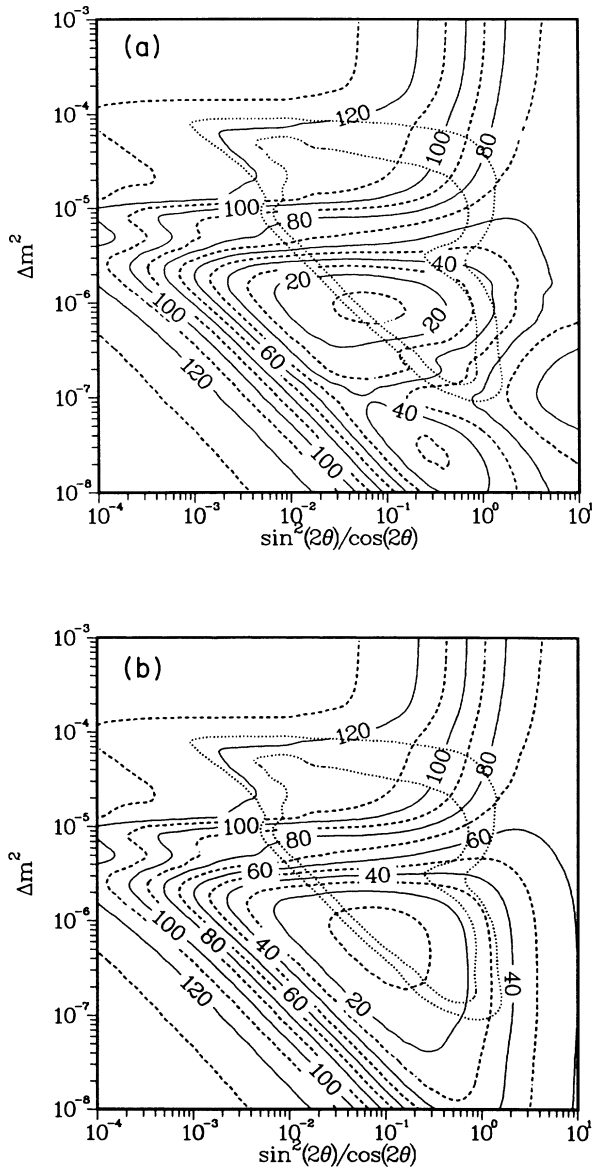


FIG. 5. Contours for the  $^{71}\text{Ga}$  experiment labeled by SNU values. The band between the dotted contours is the region consistent with the  $^{37}\text{Cl}$  results. (a) For night; (b) for day.

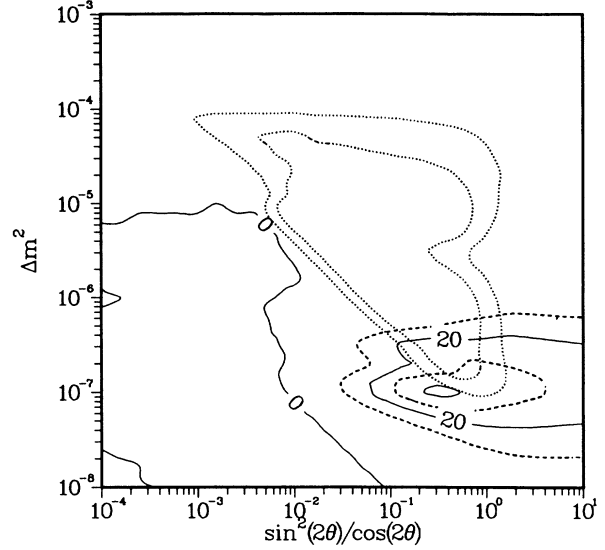


FIG. 6. Night minus day contours for the  $^{71}\text{Ga}$  experiment labeled by SNU values. The region consistent with the existing  $^{37}\text{Cl}$  experimental result of  $2.1 \pm 0.3$  SNU is shown between the dotted contours.

difference is sizable where the  $^{71}\text{Ga}$  response would be low. Therefore, if the number of counts turns out low, then the observation of a night-day difference (or lack of it) might further constrain the possible values of  $\Delta m^2$  and  $\sin 2\theta$ . In particular, for  $\Delta m^2$  of about  $10^{-7}$  and  $\sin 2\theta$  greater than about 0.3, a difference of 20 to 40 SNU's between night and day is predicted. The practical difficulty that stands in the way of such a night-day difference experiment is that presented by background and statistics, which, at low counting rates, would make a meaningful result unlikely with the present arrangements or those likely to be developed without new technology.

In short, it seems that the night-day effect could be important for the  $^{71}\text{Ga}$  experiment, but only if the counts are low relative to the solar-model predictions. However, if the counts are close to the full solar-model prediction, indicating a parameter range with little MSW effect in the Sun, there can be little MSW effect in the Earth and thus no night-day effect would be expected for the  $^{71}\text{Ga}$  experiment. The prospect for a night-day  $^{37}\text{Cl}$  experiment has been discussed recently.<sup>18</sup>

#### IV. ACCELERATOR AND COSMIC-RAY NEUTRINOS

One of the ingredients of our Eq. (2.5) for  $\bar{P}_{SE}$ , the probability that a solar neutrino remains an electron neutrino after passing through the Sun and through the Earth, is the probability  $P_{E1}$  that an electron neutrino emitted at the surface of the Earth will remain an electron neutrino after passing through it. This is, of course, the physical situation that obtains for a neutrino created at the surface of the Earth either by an accelerator or by a cosmic-ray event which then passes through a portion of the Earth to be detected at the far surface. It turns out that for the two-neutrino mixing case, by symmetry,  $P_{E1}$

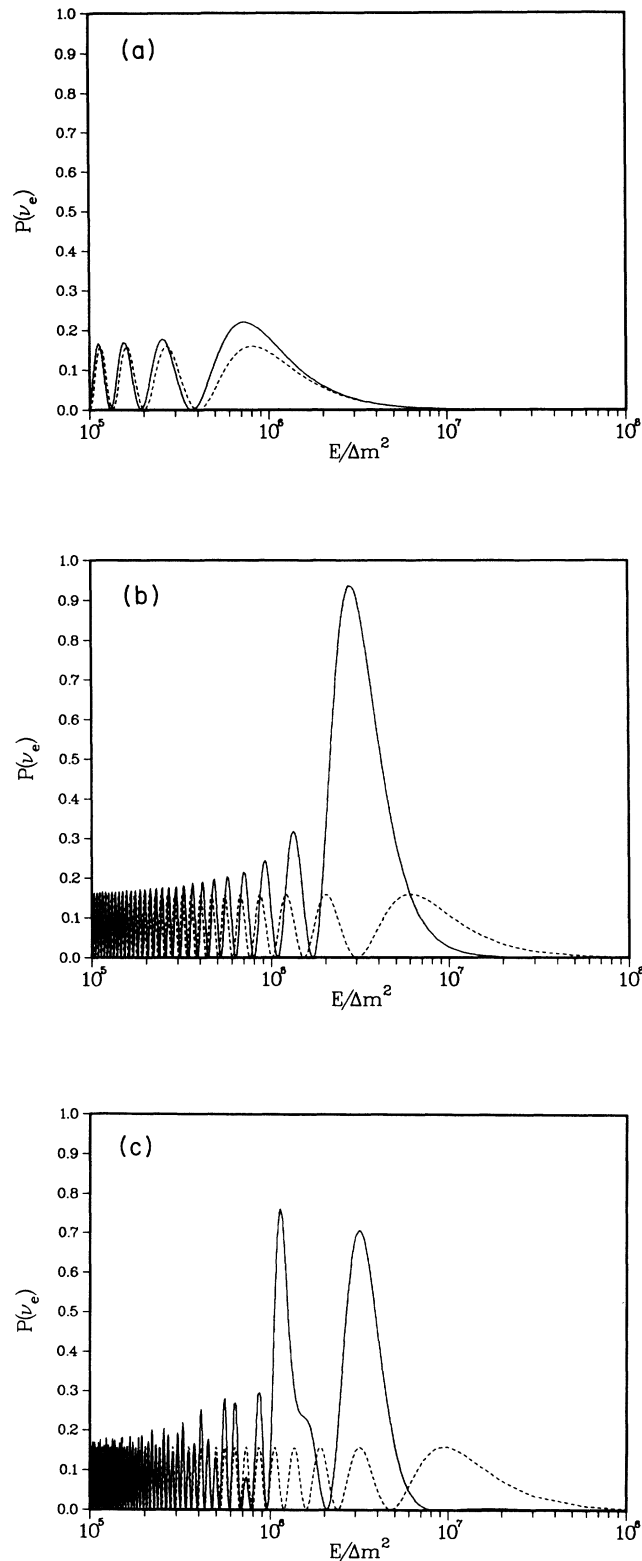


FIG. 7. (a) Probability of a muon neutrino turning into an electron neutrino after passing into the Earth and emerging at a detector 1000-km surface distance from the source.  $\sin 2\theta = 0.4$ . The solid line represents the effect of the Earth and the dashed line the replacement of the Earth's matter by vacuum. (b) and (c) are the same as (a) for a detector 8000-km (b) and 15 000-km (c) surface distance from the source.

is equally valid as the solution for the probability that a muon neutrino, for example, created at the surface of the Earth will remain a muon neutrino and not change into an electron neutrino after passing through it. This situation seems experimentally more feasible than the converse.

Figures 7(a)–(7c) show the results of calculations for the probability that a muon neutrino will change into an electron neutrino after passing through the Earth. The mixing angle  $\sin 2\theta$  was chosen to be 0.4. Figure 7(a) is a calculation for a chord which corresponds to a surface distance of 1000 km around the Earth (i.e., roughly the distance from BNL to the Sudbury detector). Oscillations in matter are just beginning to differ significantly from those that would occur in vacuum for the same distance. At short distances the matter oscillation solution approaches the vacuum solution. However, at 8000 km around the Earth, shown in Fig. 7(b), the effect of matter is dramatic for  $E(\text{MeV})/\Delta m^2(\text{eV}^2)$  in the vicinity of  $3 \times 10^6$ . The distance can be further tuned to obtain complete transformation in this region. Note, however, that the effect of the Earth is to *reduce* the transformation at high  $E/\Delta m^2$ . In contrast with these trajectories which only involve the mantle of the Earth we show in Fig. 7(c) the results of putting a detector 15 000 km around the Earth where neutrinos would go through both mantle and core. The discontinuity at the mantle-core interface (Fig. 8) results in the peculiar pattern of oscillations seen in Fig. 7(c). Thus, matter effects can be quite large for accelerator neutrinos passing through a sufficiently long Earth path. However, the number of counts obtained in any conceivable experiment at 1000 km or more is not encouraging, as has been analyzed by Murtagh.<sup>19</sup>

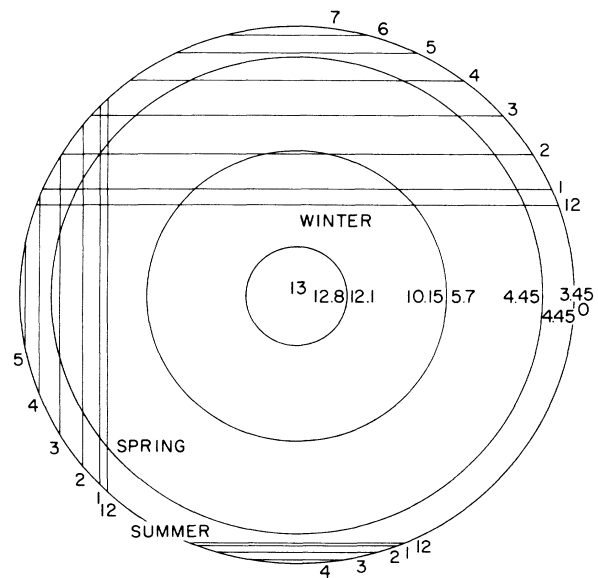


FIG. 8. Principal density zones of the Earth marked together with the densities (in  $\text{g}/\text{cm}^3$ ) at the beginning and ends of these zones. Trajectories through the Earth followed by a solar neutrino to reach a detector located at  $43^\circ$  north latitude at various times of the night at the winter and summer solstices and the spring-fall equinoxes, are also shown.



LoSecco<sup>20</sup> and collaborators have estimated that it is possible to put a rough limit on the value of  $\sin 2\theta$  from the lack of up-down asymmetry in already existing data from the Kamiokande experiment. We have calculated the full contour plot as a function of the mixing angle and mass-energy parameter for the detection of electron neutrinos that started as muon neutrinos at the surface of the Earth. Figure 9 shows a contour plot of the probability of conversion of muon into electron neutrino for all neutrinos coming from  $37^\circ$  or more below Earth's horizon (20% of the total solid angle); this corresponds to the event selection of LoSecco *et al.*<sup>20</sup> There are two regions where the transformation is large. For large mixing angles ( $\sin 2\theta$  greater than about 0.7) and  $\Delta m^2/E$  large enough there is a broad region of transformation due partially to the vacuum mixing. There is an additional island of large transformation at  $\Delta m^2/E$  of about  $3.5 \times 10^{-7}$  largely due to Earth's matter. If the detector is sensitive to neutrino energy of about 300 MeV, then for  $\Delta m^2$  of about  $10^{-4}$  and  $\sin 2\theta$  between 0.25 and 0.6, more than half of the muon neutrinos from this lower direction will change to electron neutrinos. In contrast, all the muon neutrinos produced above the detector will travel a relatively short length and remain muon neutrinos. This calculation illustrates the usefulness of the up-down

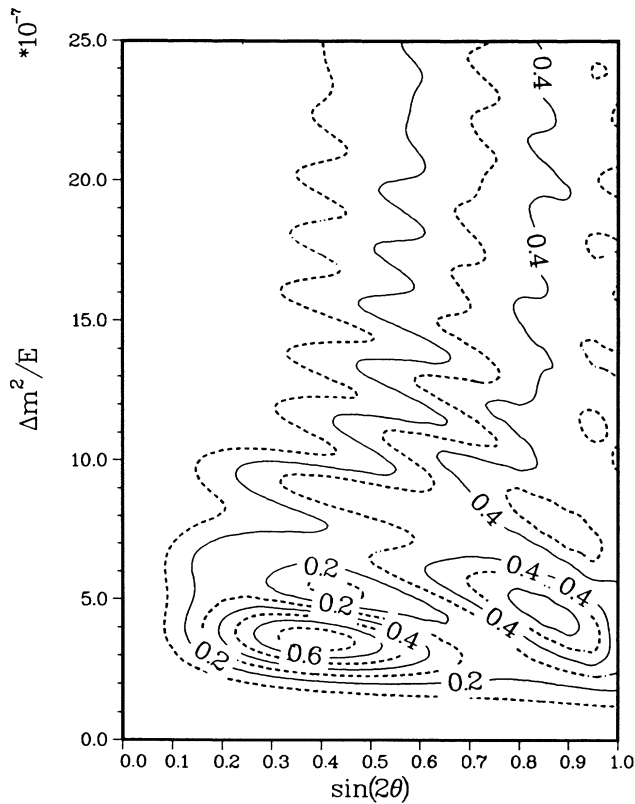


FIG. 9. Probability that muon neutrinos would change into electron neutrinos after passing through the Earth. An average of all events entering the detector from  $37^\circ$  or more below the Earth's horizon is taken. In this illustration the neutrino flux is taken as independent of angle.

asymmetry in constraining the neutrino mass and mixing angle in a limited range of these parameters. These results are in agreement with those of LoSecco *et al.*<sup>20</sup>

## V. DETECTION OF NEUTRINO SPECTRA: THE SUDBURY HEAVY-WATER DETECTOR

A large heavy-water Cherenkov detector has been proposed<sup>21</sup> that would be sensitive to the solar  $^8\text{B}$  electron neutrino flux, spectrum, and direction. In addition, the detector might also measure the  $^8\text{B}$  neutrino flux independent of flavor. We have investigated the effects of the Earth on the expected number of counts for the electron-neutrino parts of the experiment. While the effective range theory shows that a calculation of the deuterium to

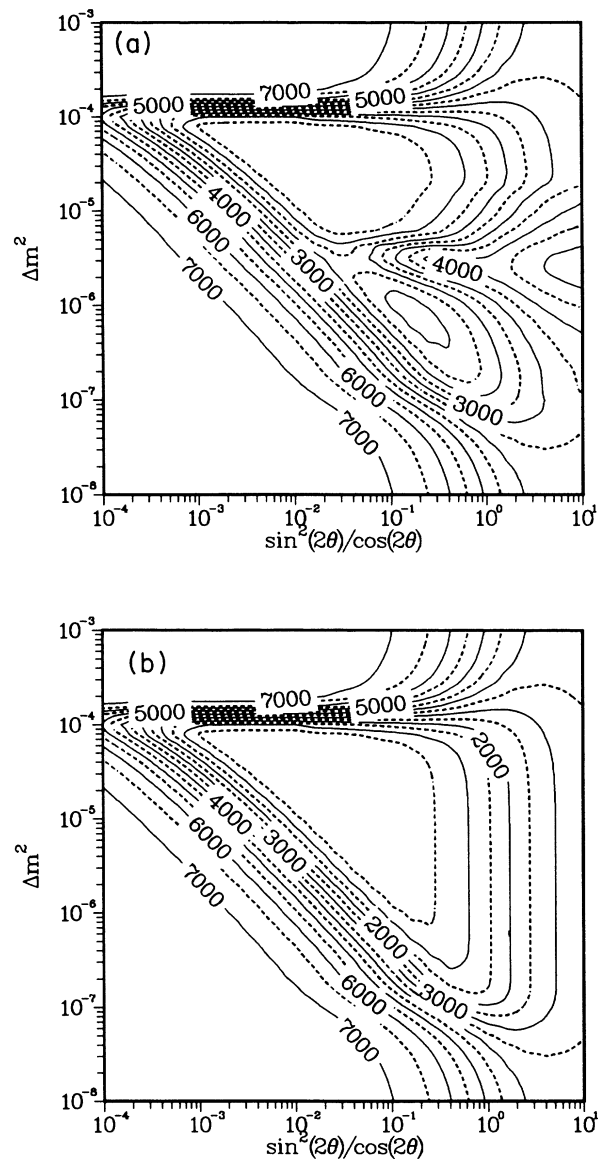


FIG. 10. Number of events per kiloton year to be detected by the Sudbury heavy-water detector as a function of  $\Delta m^2$  and  $\sin 2\theta$ . The daytime rate is shown in (b), and the spring or fall nighttime rate in (a).

$p$ - $p$  neutrino-induced transition is nearly independent of parameters,<sup>22</sup> we have found it more convenient to directly calculate the integrals numerically. A standard Yukawa interaction was taken for the  $p$ - $p$  interaction and a standard Hulthen wave function for the deuteron. Expected energy resolution of  $\sqrt{E}/2.11$  (Ref. 23) was included by folding the calculated results with a corresponding resolution function.

Figure 10 shows the daytime and nighttime number of expected counts as a function of  $\Delta m^2$  and  $\sin 2\theta$ . With an assumed threshold of 5 MeV, the detector will be sensitive only to  $^8\text{B}$  neutrinos from the Sun, with the exception of the very weak (hep) branch.<sup>6</sup> 100% triggering efficiency was assumed above 5 MeV and zero efficiency below 5 MeV. The calculation reported here contents itself with  $^8\text{B}$  neutrinos. Thus, the shape of the contours is similar to that for the  $^{37}\text{Cl}$  detector, except that the contour for  $^{37}\text{Cl}$  (Fig. 2) shows a small bump at  $\Delta m^2$  of  $10^{-5}$  (indicating the onset of an outward shift of the diagonal contours at lower  $\Delta m^2$ ), corresponding to the contribution of neutrinos between the 0.81-MeV threshold and 5 MeV. The Earth effect is clearly apparent in the distortion of contours for  $\Delta m^2 > 10^{-5}$ ,  $\sin^2 2\theta / \cos 2\theta > 10^{-2}$ .

A crucial advantage of the Sudbury experiment is that it is designed to detect the energy of the neutrinos; the proposal anticipates a precision in energy determination of 15% at 10 MeV. This makes possible the determination of the distortion of the neutrino spectrum shape. An alteration of spectrum shape is characteristic of the MSW effect, and so characteristically differentiates between alternate mechanisms for resolving the solar-neutrino problem.

Figure 11 shows the expected number of daytime counts for  $E > 9$  MeV. Not only is the number of counts reduced but also the contour shapes are shifted relative to the fuller ( $E > 5$  MeV) spectrum inclusion. Figure 12 exhibits this spectrum distortion effect as a difference of the number of low-energy events ( $5 < E < 9$  MeV) minus 3.44

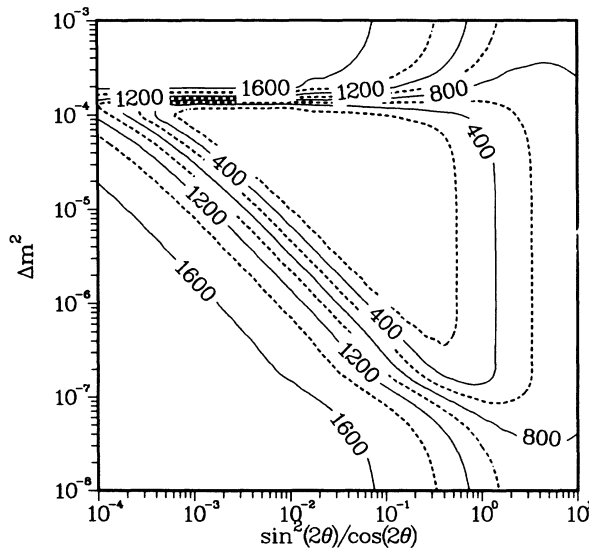


FIG. 11. As in Fig. 9, but only the high-energy daytime events.

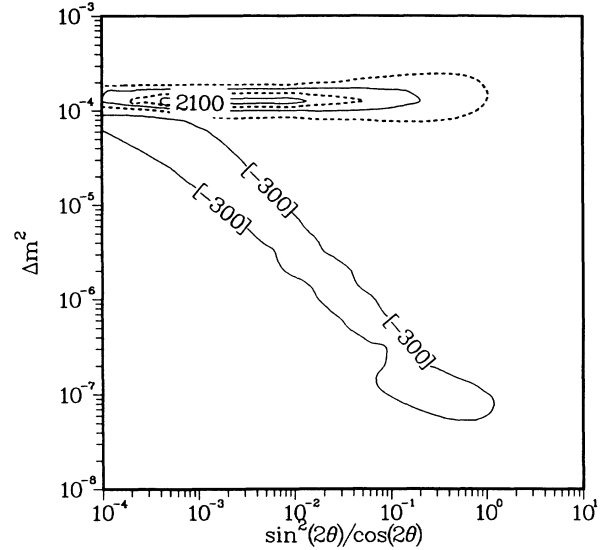


FIG. 12. Number of low-energy events ( $5 < E < 9$  MeV) minus 3.44 times the number of high-energy events ( $9 \text{ MeV} < E$ ) seen in the daytime at the Sudbury heavy-water detector. Solid contours are at  $-300, 900, 2100$ ; dashed contours are at  $300, 1500$ .

times the number of high-energy events ( $9 \text{ MeV} < E$ ). The normalization factor 3.44 has been chosen so as to make equal the number of low- and high-energy events if there were no MSW effect. Inside the diagonal contour in Fig. 12 there is a relative depletion of low-energy events relative to high-energy events. For  $\Delta m^2$  a little larger than  $10^{-4}$ , there is a relative excess of low-energy events for a broad range of  $\sin 2\theta$ . Determining such a difference in number of events experimentally might provide a constraint on allowable values of  $\Delta m^2$  and  $\sin 2\theta$ .

Of course, since this is a real-time experiment, one could use the difference between nighttime and daytime counts (such as is seen in Fig. 10) to obtain information on  $\Delta m^2$  and  $\sin 2\theta$ . In fact a real-time experiment automatically tags events by time and date, thus identifying a trajectory length with each event. This would allow the events to be binned most efficiently for isolating effects of the Earth in terms of length of matter traversed rather than some time-of-day or season-of-year variable which involves an average over a number of trajectories.

## VI. CONCLUSIONS

Our calculations have shown that for values of the two-neutrino mixing angle  $\sin 2\theta \geq 0.1$  there is a large transformation effect induced by passage through the Earth. This transformation from one species to the other (either  $\nu_\mu$  to  $\nu_e$  or vice versa) occurs in the  $E/\Delta m^2$  range of about  $1-7 \times 10^6$ . Depending on  $\Delta m^2$ , this transformation effect could turn out to provide a spectacular determination of the neutrino mass and mixing parameters. With different solar-neutrino, cosmic-ray neutrino, and accelerator-neutrino experiments probing different ranges of neutrino energy, one can hope to eventually hit on the sensitive  $E/\Delta m^2$  range for transformation in the Earth.

We would also like to make the general observation that the parameters of the solar model have a large effect on the predicted locus of the values of  $\sin 2\theta$  and  $\Delta m^2$  consistent with the  $^{37}\text{Cl}$  experiment. As was clearly seen in Fig. 2(c), there is almost no overlap at the one  $\sigma$  level between  $\Delta m^2, \theta$  determinations based on a 5.8 SNU solar model with those based on a 7.9 SNU solar model.

#### ACKNOWLEDGMENTS

We are grateful to R. Davis, Jr., G. Friedlander, M. Goldhaber, R. Hahn, W. J. Marciano, and J. K. Rowley for useful and stimulating discussions. This work was supported by U. S. Department of Energy Contract No. DE-AC02-76CH00016.

#### APPENDIX A: TREATMENT OF THE OSCILLATING TERMS

If, at the emergence from the solar medium, the neutrino state is known, its development during travel through the vacuum of space is simply given by

$$\Psi(t) = \exp \left[ \frac{-i}{\hbar} \frac{m_1^2}{2E} t \right] \cos \alpha | \nu_1 \rangle - \exp \left[ \frac{-i}{\hbar} \left( \frac{m_2^2}{2E} t + \phi \right) \right] \sin \alpha | \nu_2 \rangle ,$$

where  $\phi$  is the constant phase angle, and  $\alpha$  is defined by the fraction in components 1 or 2. Then expectation values will involve a cross term proportional to

$$\exp \left[ \frac{i}{\hbar} \left( \frac{\Delta m^2}{2E} t + \phi \right) \right] .$$

Thus, the probability fraction of a neutrino remaining of the electron type after transmission through the Earth,  $P_{\text{SE}}$ , will involve such oscillating terms. This appendix examines whether we are justified in discarding them; in particular, the "sharp" lines in the solar-neutrino spectrum need special scrutiny.

The terms proportional to

$$\exp \left[ \pm \frac{i}{\hbar} \left( \frac{\Delta m^2}{2E} t + \phi \right) \right]$$

are rapidly oscillating; thus, the phase

$$\chi = 2\pi \left[ \frac{\Delta m^2}{4\pi E} \frac{t}{\hbar} \right]$$

can, in general, be seen to involve many multiples of  $2\pi$ . Taking  $t$  as the Earth-Sun distance,  $\sim 1.5 \times 10^{13}$  cm,  $E/\Delta m^2 \sim 10^5$  MeV/eV<sup>2</sup>,  $\chi \sim 2\pi \times 10^6$ ;  $E/\Delta m^2 \sim 10^8$  MeV/eV<sup>2</sup>,  $\chi \sim 2\pi \times 10^3$ . Since in any realizable solar-neutrino experiment there will necessarily be averaging over each of the parameters that enter  $\chi$ , the energy and distance, it is sensible to examine the degree to which this averaging reduces the rapidly oscillating terms to negligible factors.

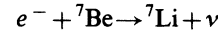
Variation in the distance  $t$  occurs because the solar source size is finite, the Earth-Sun orbit is elliptical, and

the Earth rotates. The latter two are part of the time-of-day and time-of-year effects here and should not be averaged away. The solar source sizes must be averaged over. The standard-solar-model calculations of Bahcall and Ulrich<sup>6</sup> result in a radial profile for each of the important neutrino sources. The most centrally distributed is the  $^8\text{B}$  source. The effective  $^7\text{Be}$  neutrino source strength is distributed over somewhat greater distances, and is very roughly described by

$$(\Delta t)^2 e^{-(\Delta t/\sigma)^2}, \quad \sigma \sim 0.06 R_\odot ,$$

where  $\Delta t$ , the distance from the solar center, is measured along the straight line transit to the detector. The  $p$ - $p$  flux source size is larger still, very roughly twice that of the  $^7\text{Be}$ .

The range of energies over which it is appropriate to average the continuous fluxes, such as  $p$ - $p$  or  $^8\text{B}$ , is determined by the energy resolution of the experiment. Radiochemical experiments have, of course, very wide energy acceptance. The present spectrum of proposed counter detectors envisage resolutions in the MeV range, to be compared to the  $\sim 10$  MeV midregion of the  $^8\text{B}$  neutrino spectrum; as we shall see, exact specifications on this point are not really required for this question of the oscillating terms. The sharp line spectra, such as the  $^7\text{Be}$  lines, are in a somewhat different class. While no immediate experiment will put very important weight on these neutrinos, it is worth analyzing them against some future possibility. For definiteness we consider the more energetic and populous higher-energy  $^7\text{Be}$  line. The basic reaction



is broadened by the spread in energies of the incoming electron and by the Doppler spreading that comes about from the velocities of the thermalized  $^7\text{Be}$  ions. The electrons are captured, in largest fraction, directly from the plasma, and, in smaller measure, from the bound atomic states; to simplify the discussion here we consider only the capture from the plasma, assuming a pure Boltzmann distribution for the electron energies. The spread of neutrino energies is, then, to lowest order

$$\Delta E_\nu \simeq T_e + \frac{\mathbf{v}_7 \cdot \hat{\mathbf{k}}}{c} E_\nu(0) ;$$

$T_e$  is the electron kinetic energy,  $\mathbf{v}_7 \cdot \hat{\mathbf{k}}$  the component along the neutrino direction of the velocity of the  $^7\text{Be}$  in the plasma, and  $E_\nu(0)$  is the line-center neutrino energy. We can approximate the dependence of the  $^7\text{Be}$  neutrino production rate on electron energy by a simple  $1/v_e$  factor, on recalling that the Coulomb enhancement goes as  $1/v_e^2$  and the flux is proportional to  $v_e$ . We will not consider collision broadening, which we guess to be much smaller.

The effects on the oscillating terms for such a "sharp line" are, then, obtained by evaluating simple expressions of the form

TABLE II. Treatment of the oscillating terms. Numerical evaluation for some “averaging” factors, using the sample values  $t_0 = 1.5 \times 10^{13}$  cm,  $kT = 1$  keV,  $E_\nu(0) = 0.8$  MeV,  $\sigma = 0.06 R_\odot \sim 4 \times 10^9$  cm,  $M_7 c^2 = 7 \times 10^3$  MeV.

$E_\nu(0)/\Delta m^2 \left[ \frac{\text{MeV}}{\text{eV}^2} \right]$	$\chi_0$	$\left[ 1 - \frac{\chi_0^2 \sigma^2}{2t_0^2} \right] \exp \left[ -\frac{\chi_0^2 \sigma^2}{4t_0^2} \right]$	$\frac{1}{\left[ 1 + \left[ \frac{kT}{E_\nu(0)} \chi_0 \right]^2 \right]^{1/2}}$	$\exp \left[ -\frac{\chi_0^2 kT}{2M_7 c^2} \right]$
$10^5$	$4 \times 10^6$	0	$2 \times 10^{-4}$	0
$10^6$	$4 \times 10^5$	0	$2 \times 10^{-3}$	0
$10^7$	$4 \times 10^4$	$-4 \times 10^{-11}$	$2 \times 10^{-2}$	0
$10^8$	$4 \times 10^3$	0.3	$2 \times 10^{-1}$	0.3
$10^9$	$4 \times 10^2$	1	0.9	1

$$\begin{aligned}
 & \int d(\Delta t) v_e^2 dv_e dv_\gamma \cos \chi_0 \left[ 1 + \frac{\Delta t}{t_0} + \frac{T_e}{E_\nu(0)} + \frac{v_\gamma}{c} \right] (\Delta t)^2 e^{-(\Delta t/\sigma)^2} e^{-m_e v_e^2/2kT} / v_e e^{-M_7 v_\gamma^2/2kT} \\
 & \quad \int d(\Delta t) v_e^2 dv_e dv_\gamma (\Delta t)^2 e^{-(\Delta t/\sigma)^2} e^{-m_e v_e^2/2kT} / v_e e^{-M_7 v_\gamma^2/2kT} \\
 & \quad = \left[ \left[ 1 - \frac{\chi_0^2 \sigma^2}{2t_0^2} \right] e^{-\chi_0^2 \sigma^2/4t_0^2} \frac{1}{\left[ 1 + \left[ \frac{kT}{E_\nu(0)} \chi_0 \right]^2 \right]^{1/2}} \exp \left[ -\frac{\chi_0^2}{2} \frac{kT}{M_7 c^2} \right] \right] \cos(\chi_0 + \delta), \\
 & \quad \delta = \arctan \left[ \frac{kT}{E_\nu(0)} \chi_0 \right].
 \end{aligned}$$

Some sample numerical values for the various factors appearing in the above expression are listed in Table II, and it is immediately seen that for values of the important parameter  $E_\nu(0)/\Delta m^2$  smaller than  $10^8$  MeV/eV<sup>2</sup> the oscillating terms may be discarded without fear of losing more than  $\pm 0.02$  in  $\bar{P}_{SE}$ . This is the  $E/\Delta m^2$  range of interest in this paper; should one need to go beyond this, care must be taken for those experiments in which “sharp” neutrino lines are important.

For the contributions of the continuum spectra, the relevant averaging takes the form

$$\begin{aligned}
 & \int d(\Delta E) \cos \chi_0 \left[ 1 + \frac{\Delta E}{E_\nu(0)} \right] e^{-(\Delta E/F)^2} \\
 & \quad = \exp \left[ -\frac{\chi_0^2}{4} \left[ \frac{\Gamma}{E_\nu(0)} \right]^2 \right] \cos \chi_0.
 \end{aligned}$$

It is clear that even for  $E_\nu(0)/\Delta m^2 = 10^9$  MeV/eV<sup>2</sup>,  $\chi_0 \sim 4 \times 10^2$ , a resolution width,  $\Gamma/E_\nu(0)$  of  $\sim 1\%$  or greater is sufficient to reduce the amplitude to  $\sim 0.02$ ; for

$E/\Delta m^2 = 10^8$ ,  $\Gamma/E_\nu(0) \sim 1\%$  leads to the minute  $e^{-400}$  amplitude. We need not concern ourselves with this problem for the foreseeable future.

## APPENDIX B: DERIVATION OF THE BASIC TRANSMISSION EQUATION

The basic equation describing the transmission through matter of neutrinos that can mix has been given by Wolfenstein.<sup>7</sup> In this section, the connection between this transmission equation and the underlying Dirac equation is laid out in pedagogically explicit form. Only the case of two-neutrino mixing is considered here, and we limit ourselves to Dirac neutrinos and a simple interaction.

In the Wolfenstein formalism the general state, a mixture of the two neutrino species  $|\nu_e\rangle$  and  $|\nu_X\rangle$ ,

$$\Psi(t) = C_e(t) |\nu_e\rangle + C_X(t) |\nu_X\rangle$$

obeys the transmission equation

$$i \frac{d}{dt} \begin{bmatrix} C_e \\ C_X \end{bmatrix} = \begin{bmatrix} \frac{m_1^2}{2E} \cos^2 \theta + \frac{m_2^2}{2E} \sin^2 \theta + \sqrt{2} G_F n_e & \left[ \frac{m_2^2}{2E} - \frac{m_1^2}{2E} \right] \sin \theta \cos \theta \\ \left[ \frac{m_2^2}{2E} - \frac{m_1^2}{2E} \right] \sin \theta \cos \theta & \frac{m_2^2}{2E} \cos^2 \theta + \frac{m_1^2}{2E} \sin^2 \theta \end{bmatrix} \begin{bmatrix} C_e \\ C_X \end{bmatrix}. \quad (\text{B1})$$

The  $|\nu_e\rangle$  and  $|\nu_X\rangle$  are the particular combinations of the mass eigenstates  $|\nu_1\rangle$  and  $|\nu_2\rangle$  that couple to the  $\beta$  decay and other weak interactions; the  $\theta$  angle describes this fundamental mixing

$$|\nu_e\rangle = \cos\theta |\nu_1\rangle + \sin\theta |\nu_2\rangle, \quad |\nu_X\rangle = -\sin\theta |\nu_1\rangle + \cos\theta |\nu_2\rangle. \quad (\text{B2})$$

To derive this form, we begin with a two-channel Dirac equation for a state of energy  $E$ . It is conceptually easier to begin in terms of the mass eigenstates

$$\begin{aligned} \Psi &= \Psi_1(x) |\nu_1\rangle + \Psi_2(x) |\nu_2\rangle, \\ E\Psi_1 &= \left[ \frac{\hbar}{i} \alpha_x \frac{\partial}{\partial x} + \beta m_1 + V_{11} \right] \Psi_1 + V_{12} \Psi_2, \\ E\Psi_2 &= \left[ \frac{\hbar}{i} \alpha_x \frac{\partial}{\partial x} + \beta m_2 + V_{22} \right] \Psi_2 + V_{12} \Psi_1, \end{aligned} \quad (\text{B3})$$

where  $V$  represents the interaction with the medium. With the charged-current interaction

$$\begin{aligned} V &= \sqrt{2} G_F n_e |\nu_e\rangle \langle \nu_e| \\ &= \sqrt{2} G_F n_e (\cos^2\theta |\nu_1\rangle \langle \nu_1| + \sin\theta \cos\theta |\nu_1\rangle \langle \nu_2| + \sin\theta \cos\theta |\nu_2\rangle \langle \nu_1| + \sin^2\theta |\nu_2\rangle \langle \nu_2|) \\ &= V_{11} |1\rangle \langle 1| + V_{12} (|1\rangle \langle 2| + |2\rangle \langle 1|) + V_{22} |2\rangle \langle 2|. \end{aligned} \quad (\text{B4})$$

For our purposes here, limitation to a one spatial dimension suffices.

The complexities of keeping the full Dirac spinor are unnecessary baggage for the present problem to the order of approximation needed. To avoid these, write

$$\Psi_1 = C_1(x) \phi_1(x), \quad \Psi_2 = C_2(x) \phi_2(x), \quad (\text{B5})$$

where  $\phi_1(x)$ ,  $\phi_2(x)$  are Dirac spinors that satisfy

$$(\alpha_x \{ [E - V_{ii}(x)]^2 - m_i^2 \}^{1/2} + \beta m_i + V_{ii}) \phi_i(x) = E \phi_i(x). \quad (\text{B6a})$$

The  $\phi_i(x)$  are of the form of free particle solutions corresponding to a "local energy"  $[E - V_{ii}(x)]$ ; in detail they are

$$\begin{aligned} \phi_i(x) &= \left[ \frac{[E - V_{ii}(x)] + m_i}{2[E - V_{ii}(x)]} \right]^{1/2} \\ &\times \left[ \frac{\xi}{\{ [E - V_{ii}(x)]^2 - m_i^2 \}^{1/2}} \sigma_x \xi \right], \end{aligned} \quad (\text{B6b})$$

where  $\xi$  is the appropriate Pauli spinor. Insertion into the defining Eq. (B3) is simplified by first noting that

$$\hbar \frac{\partial \phi(x)}{\partial x} \sim \frac{\hbar \frac{\partial V}{\partial x}}{E - V + m} \frac{m}{E - V} \phi; \quad (\text{B7})$$

this is to be compared with the orders of magnitude that are seen directly in (B3),  $V\phi$ , and also that to be obtained later for  $\hbar(\partial C/\partial x)\phi$ :

$$\frac{\hbar \frac{\partial V}{\partial x}}{E - V + m} \frac{m}{E - V} / V \sim \frac{\hbar}{E} \frac{m}{E} \frac{1}{R_{\text{scale}}}. \quad (\text{B8})$$

$R_{\text{scale}}$  is a measure of the macroscopic distance scale over which  $V$  changes, while  $\hbar/E$  is the microscopic wavelength of the neutrino. [This order of smallness is not to be confused with the adiabaticity parameter,  $((m_2^2 - m_1^2)/E)R_{\text{scale}}$ .] Neglecting terms of this order leaves (B3) in the form

$$\begin{aligned} EC_1\phi_1 &= \frac{\hbar}{i} \frac{\partial C_1}{\partial x} \alpha_x \phi_1 + (\beta m_1 + V_{11}) C_1 \phi_1 + V_{12} C_2 \phi_2, \\ EC_2\phi_2 &= \frac{\hbar}{i} \frac{\partial C_2}{\partial x} \alpha_x \phi_2 + (\beta m_2 + V_{22}) C_2 \phi_2 + V_{12} C_1 \phi_1. \end{aligned} \quad (\text{B9a})$$

Multiplying both sides by  $\alpha_x$  and rearranging, results in

$$\begin{aligned} \frac{\hbar}{i} \frac{\partial C_1}{\partial x} \phi_1 &= [(E - V_{11})^2 - m_1^2]^{1/2} C_1 \phi_1 - V_{12} C_2 \alpha_x \phi_2, \\ \frac{\hbar}{i} \frac{\partial C_2}{\partial x} \phi_2 &= [(E - V_{22})^2 - m_2^2]^{1/2} C_2 \phi_2 - V_{12} C_1 \alpha_x \phi_1. \end{aligned} \quad (\text{B9b})$$

Next, we note that, since, to order  $V$ ,

$$V_{12} \alpha_x \phi_2 \simeq V_{12} \phi_1 + \text{higher orders},$$

$$V_{21} \alpha_x \phi_1 \simeq V_{21} \phi_2 + \text{higher orders},$$

we can drop the explicit spinor dependence. Finally with

$$[(E - V_{ii})^2 - m_i^2]^{1/2} \simeq E - V_{ii} - \frac{m_i^2}{2E},$$

$$\frac{\hbar}{i} \frac{\partial C_1}{\partial x} = \left[ E - V_{11} - \frac{m_1^2}{2E} \right] C_1 - V_{12} C_2, \quad (\text{B10a})$$

$$\frac{\hbar}{i} \frac{\partial C_2}{\partial x} = \left[ E - V_{22} - \frac{m_2^2}{2E} \right] C_2 - V_{12} C_1,$$

or, in more compact form,

$$\frac{\hbar}{i} \frac{\partial}{\partial x} \begin{bmatrix} C_1 \\ C_2 \end{bmatrix} = \begin{bmatrix} E - V_{11} - \frac{m_1^2}{2E} & -V_{12} \\ -V_{12} & E - V_{22} - \frac{m_2^2}{2E} \end{bmatrix} \begin{bmatrix} C_1 \\ C_2 \end{bmatrix}, \quad (\text{B10b})$$

$$\Psi(x) = C_1(x) \phi_1(x) | \nu_1 \rangle + C_2(x) \phi_2(x) | \nu_2 \rangle. \quad (\text{B10c})$$

The definitions of the  $\phi_1(x)$ ,  $\phi_2(x)$  were, in fact, dictated by the requirement that there be no spinor dependence left; from (B9a) this can be seen as the requirements

$$\alpha_x (E - \beta_{m_i} - V_{ii}) \phi_i = \lambda_i(x) \phi_i, \quad \alpha_x \simeq \phi, \quad (\text{B11})$$

which are achieved in the “local free” solutions used above.

The final step in the derivation of Eq. (B1) follows on noting that we can generally drop the  $m/E$  and  $mV/E^2$  dependence of  $\phi_1$  and  $\phi_2$  in their appearance in the composite final wave function, Eq. (B10c). This, at first sight, appears to contradict the careful husbanding of terms in deriving the equations for  $C_1(x)$ ,  $C_2(x)$ . However the  $C_1(x)$ ,  $C_2(x)$  are quantities that will vary in magnitude between 0 and 1; the very small terms dropped from  $\phi_1$ ,  $\phi_2$  are never amplified in their effects in  $\Psi(x)$  or expectation values formed with it. On the other hand, the whole dependence of  $C_1(x)$ ,  $C_2(x)$  depends on the small terms

that are amplified by the large transmission distances; this is easily seen in the trivial example provided by solving (B10a) with  $V_{12}=0$ , and  $C_1(0)=1$ :

$$C_1(x) = \exp \left[ \frac{i}{\hbar} \left( -V_{11} - \frac{m_1^2}{2E} \right) x \right],$$

$$C_2(x) = \exp \left[ \frac{i}{\hbar} \left( -V_{22} - \frac{m_2^2}{2E} \right) x \right] - 1,$$

the inconsequential common phase factor  $e^{(i/\hbar)Ex}$  having been dropped. The error incurred in the overall wave function in dropping the  $mV/E^2$ ,  $m/E$  terms from  $\phi_1$ ,  $\phi_2$  are only of order  $mV/E^2$ ,  $m/E$ ; it is an order we will not discuss here.

With this final simplification (B10c) becomes

$$\Psi(x) = [C_1(x) | \nu_1 \rangle + C_2(x) | \nu_2 \rangle] \phi(x), \quad (\text{B10d})$$

where  $\phi(x)$  is the  $V=0$ ,  $m=0$  common version of  $\phi_1$ ,  $\phi_2$ . Rotation between the  $| \nu_1 \rangle$ ,  $| \nu_2 \rangle$  and the  $| \nu_e \rangle$ ,  $| \nu_\mu \rangle$  basis now immediately puts Eqs. (B10a) and (B10d) in the form (B1)—except for two trivial points: (1) The diagonal term equal to  $E \times (\text{unit matrix})$  in Eq. (B10b) can be dropped or removed by a common phase factor; (2) the change of coordinate variable  $x \rightarrow t$ , it being understood that units of  $c=1$  are in use.

- <sup>1</sup>S. P. Mikheyev and A. Yu. Smirnov, *Yad. Fiz.* **42**, 1441 (1985) [*Sov. J. Nucl. Phys.* **42**, 913 (1985)]; L. Wolfenstein, *Phys. Rev. D* **20**, 2634 (1979), also see Ref. 7; H. A. Bethe, *Phys. Rev. Lett.* **56**, 1305 (1986); S. P. Rosen and J. M. Gelb, *Phys. Rev. D* **34**, 969 (1986).
- <sup>2</sup>J. K. Rowley, B. T. Cleveland, and R. Davis, Jr., in *Solar Neutrinos and Neutrino Astronomy (Lead High School, Lead, South Dakota)*, proceedings of a Conference, sponsored by Homestake Mining Company, edited by M. L. Cherry, K. Lande, and W. A. Fowler (AIP Conf. Proc. No. 126) (AIP, New York, 1984).
- <sup>3</sup>A. J. Baltz and J. Weneser, *Phys. Rev. D* **35**, 528 (1987).
- <sup>4</sup>E. D. Carlson, *Phys. Rev. D* **34**, 1454 (1986); J. Bouchez, M. Cribier, W. Hampel, J. Rich, M. Spiro, and D. Vignaud, *Z. Phys. C* **32**, 499 (1986).
- <sup>5</sup>W. C. Haxton, *Phys. Rev. Lett.* **57**, 1271 (1986); Stephen J. Parke, *ibid.* **57**, 1275 (1986); Stephen J. Parke and Terry P. Walker, *ibid.* **57**, 2322 (1986).
- <sup>6</sup>John N. Bahcall and Roger K. Ulrich, *Rev. Mod. Phys.* **60**, 297 (1988).
- <sup>7</sup>L. Wolfenstein, *Phys. Rev. D* **17**, 2369 (1978).
- <sup>8</sup>F. D. Stacy, *Physics of the Earth*, 2nd Ed. (Wiley, New York, 1985), p. 171; J.-C. De Bremaecker, *Geophysics: The Earth's Interior* (Wiley, New York, 1985), p. 63.
- <sup>9</sup>S. P. Mikheyev and A. Yu. Smirnov, in *New and Exotic Phenomena*, proceedings of the Moriond Workshop, Les Arcs, Savoie, France, 1987, edited by O. Fackler and J. Tran Thanh

- Van (Editions Frontières, Gif-sur-Yvette, France, 1987).
- <sup>10</sup>W. C. Haxton, *Phys. Rev. D* **35**, 2352 (1987).
- <sup>11</sup>P. Pizzochero, *Phys. Rev. D* **36**, 2293 (1987).
- <sup>12</sup>S. T. Petcov, *Phys. Lett. B* **191**, 299 (1987).
- <sup>13</sup>S. Toshev, *Phys. Lett. B* **196**, 170 (1987).
- <sup>14</sup>A. J. Baltz and J. Weneser, Proceedings of the BNL Neutrino Workshop, 1987 (BNL Report No. 52079), p. 121.
- <sup>15</sup>J. N. Bahcall, B. T. Cleveland, R. Davis, Jr., and J. K. Rowley, *Astrophys. J.* **292**, L79 (1985).
- <sup>16</sup>J. Mathews and R. L. Walker, *Mathematical Methods of Physics* (Benjamin, New York, 1965), p. 336.
- <sup>17</sup>T. Kirsten, in *Neutrino '86: Neutrino Physics and Astrophysics*, proceedings of the 12th International Conference, Sendai, Japan, 1986, edited by T. Kitagaki and H. Yuta (World Scientific, Singapore, 1986), p. 317; I. R. Barabanov *et al.*, in *Solar Neutrinos and Neutrino Astronomy* (Ref. 2), p. 175.
- <sup>18</sup>M. L. Cherry and K. Lande, *Phys. Rev. D* **36**, 3571 (1987).
- <sup>19</sup>M. Murtagh, Proceedings of the BNL Neutrino Workshop, 1987 (Ref. 14), p. 81.
- <sup>20</sup>J. M. LoSecco, *Phys. Rev. Lett.* **57**, 652 (1986); J. M. LoSecco *et al.*, *Phys. Lett. B* **184**, 305 (1987).
- <sup>21</sup>The Sudbury Neutrino Observatory Collaboration, G. Aardsmas *et al.*, *Phys. Lett. B* **194**, 321 (1987); G. T. Ewan *et al.*, Report No. SNO-87-12, 1987 (unpublished).
- <sup>22</sup>F. J. Kelly and U. Uberall, *Phys. Rev. Lett.* **16**, 145 (1966).
- <sup>23</sup>M. Sardesai (private communication).